Pergamon

Available online at www.sciencedirect.com

SCIENCE @ DIRECT®

Cement and Concrete Research 34 (2004) 927–934

CEMENT AND CONCRETE RESEARCH

Development of thermal energy storage concrete

Dong Zhang[a,*], Zongjin Li[b], Jianmin Zhou[a], Keru Wu[a]

[a]*State Key Laboratory of Concrete Materials Research, School of Materials Science and Engineering, Tongji University, 1239 Siping Road, Shanghai 200092, China*

[b]*Department of Civil Engineering, Hong Kong University of Science and Technology, Clear Water Bay, Kowloon, Hong Kong SAR, China*

Received 21 April 2003; accepted 30 October 2003

Abstract

In this paper, a two-step procedure to produce thermal energy storage concrete (TESC) is described. At the first step, thermal energy storage aggregates (TESAs) were made from porous aggregates absorbing phase changing materials (PCMs). At the second step, TESC was produced with a normal mixing method and using TESAs. An adequate amount of PCM can be incorporated into concrete by the two-step procedure. It can be seen experimentally that the energy storage capacity of the TESC was comparable with that of a commercially available PCM. The experimental results showed that the geometrical features of the porous structure of the aggregates had significant effect on their absorbing ability of the PCM. Aggregates with large pore connectivity factor and transport tunnel in boundary part can absorb more PCM. It was also found that the phase changing behavior was affected by the volume fraction of PCM in concrete.

Keywords: Image analysis; Mercury porosimetry; Thermal analysis; Concrete; Thermal energy storage

1. Introduction

Fast worldwide economic development leads to a quickly increasing energy demand. However, conventional fossil energy sources are limited, and their use is related to emission of harmful gases, which are responsible for climate changes and environmental pollution. To cope with this challenging situation, energy should be used more efficiently. Building energy consumption accounts for more than one third of total primary energy consumption in many countries. Improving the energy efficiency of buildings is an effective way to improve the total energy efficiency of a society and has significant benefit for the economy.

Methods of improving the energy efficiency of buildings can be divided into two categories: passive and active methods. Passive methods improve the energy efficiency of a building by using materials with low thermal conductivity. Active methods enhance the energy efficiency of a building by using materials with high thermal energy storage capacity. Recently, investigation of the active methods has become one of the hottest topics in the fields of thermal energy engineering and building industry. Results of Hirayama et al.'s study [1] indicated that using high thermal energy storage materials in a building cannot only reduce its energy cost and scale of the air-conditioning systems, but can also flatten the fluctuation of indoor temperature and improve the indoor thermal environment.

Thermal energy storage methods can be further divided into two subcategories: sensible thermal energy and latent thermal energy storage methods [2]. Examples of sensible thermal energy storage method in buildings are the water wall and Trombe wall, which are based on specific heat of materials and temperature variation; their energy storage capacity is far less than that of the latent thermal energy storage method. For example, water has a specific heat of 4.2 J/g °C, which is higher than that of most building materials, but the latent heat of most materials is in the range of several tens to several hundreds of joules per gram. For example, the latent heat of paraffin wax is 173.6 J/g. Besides the building industry, the latent thermal energy storage method has been used in many other fields [3–5].

The materials used for latent thermal energy storage are phase changing materials (PCMs). Early research on PCMs and the latent thermal energy storage method in buildings was initiated by the Office of Solar Energy of the Department of Energy of the United States in 1982 [6]. Latent thermal

---

* Corresponding author. Tel.: +86-21-65980527; fax: +86-21-65980530.

E-mail address: zhangdng@mail.tongji.edu.cn (D. Zhang).

0008-8846/$ – see front matter © 2004 Elsevier Ltd. All rights reserved.
doi:10.1016/j.cemconres.2003.10.022

Table 1
Basic properties of butyl stearate

Melting temperature (°C)	Boiling temperature (°C)	Density at 25 °C (g/cm^3)	Viscosity at 25 °C (cP)
18	220	0.85	7

energy storage is also the key part in Annex 10 in the project of Energy Conservation through Energy Storage (ECES 1998) financially supported by the International Energy Agency (IEA) [7]. Many researchers have proven the effectiveness of PCMs in improving the energy efficiency and indoor thermal comfort of buildings based on numerical simulations [8–11]. Besides the theoretical works, experimental studies on the performance of PCMs in buildings were also conducted and reported. Some researchers incorporated PCMs into common wall materials for storing solar energy [12,13]. Others added organic PCMs in building materials [14,15]. Hawes et al. experimentally studied the thermal performance of wall materials containing PCMs [16].

One of the main difficulties in the development of building materials containing PCMs is incorporation of PCMs in matrix materials. Some researchers used building material products, such as concrete bricks and gypsum wallboards, directly as the matrix materials of PCMs. This method needs additional treatments on the surface of the products to prevent PCM from flowing out and polluting the indoor environment [17], which results in high cost of the final products. Moreover, it is difficult to incorporate a sufficient amount of PCM in building materials by this method.

In this paper, a two-step procedure for incorporation of PCM in building materials is proposed. First, thermal energy storage aggregates (TESAs) were made from porous aggregates and liquid PCM by vacuum impregnation. Then thermal energy storage concrete (TESC) was produced using TESAs, Portland cement, and other raw materials of normal concrete. The two-step method made use of the high porosity of porous aggregates to achieve sufficient storage of PCM in concrete, and had the dense cement-based

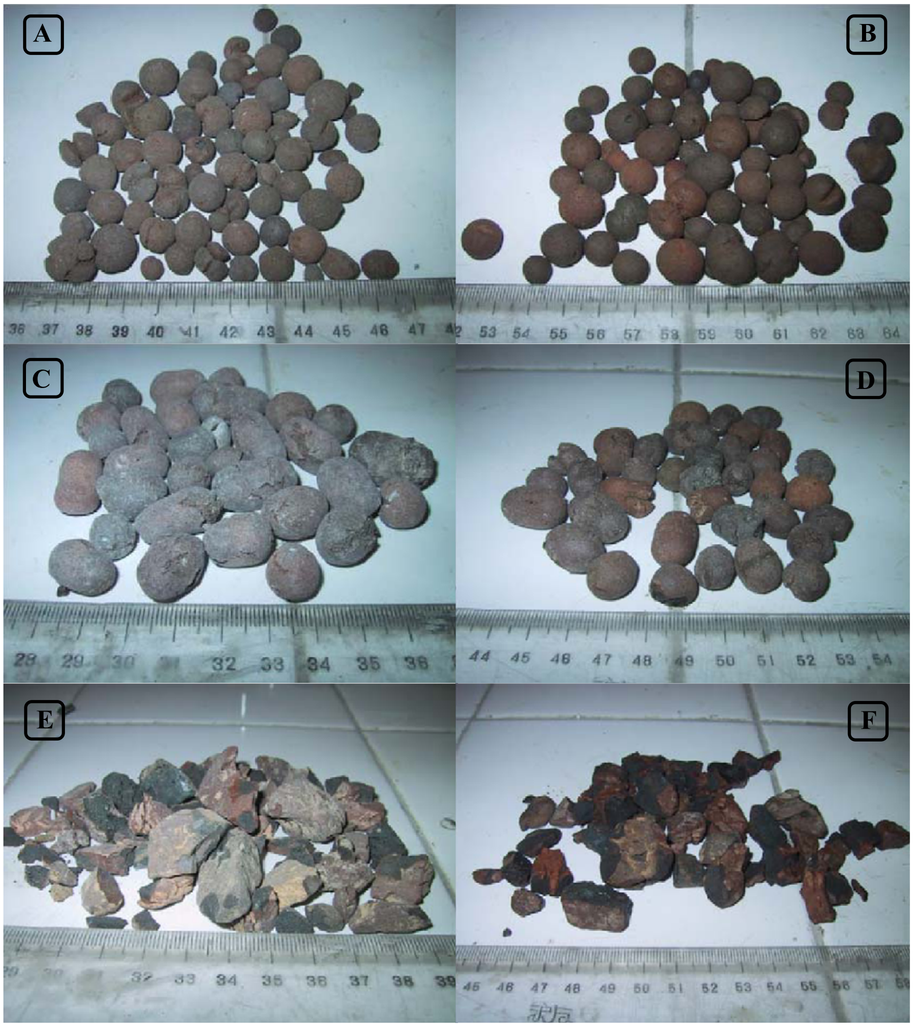

Fig. 1. Porous aggregates before and after absorbing PCM.

materials surround the porous aggregates to avoid the outflow and pollution of PCM. In this study, the feasibility of the two-step method and the effect of the porous structure of the aggregates on their PCM-absorbing capacity and thermal behavior of the TESC were investigated. Comparison of the thermal energy storage capacity of the concrete with that of a commercially available PCM indicated that TESC has a good application potential in the field of building energy conservation.

2. Experiment

2.1. Materials

In the research, three kinds of materials were used. They are listed as follows.

2.1.1. Phase changing material

Butyl stearate (BS), a type of organic PCM, was used. Its basic properties are shown in Table 1.

2.1.2. Porous materials

Porous aggregates, including one kind of expanded shale aggregate and two kinds of expanded clay aggregates, were used as supporting materials of PCM. Fig. 1 shows images of these materials. A and B are images of an expanded clay aggregate, Superlite. A is plain aggregate, and B is aggregate impregnated with PCM. C and D are images of another kind of expanded clay aggregate, normal clay aggregate. C is plain aggregate, and D is aggregate impregnated with PCM. E and F are images of expanded shale aggregate. E is plain aggregate, and F is aggregate impregnated with PCM. In the following sections, Superlite clay aggregate, normal clay aggregate, and shale aggregate are denoted by C1, C2, and S, respectively. Table 2 shows the properties of these porous aggregates.

2.1.3. Matrix materials

Ordinary Portland cement, sand with fineness modulus of 2.65 and water were used to form the concrete matrix.

2.2. Two-step procedure to produce TESC

2.2.1. Thermal energy storage aggregates

It can be seen in Table 2 that although the porous aggregates had high porosity, from 34% to 75%, it was very difficult for them to absorb large quantity of liquid (water) by simple immersion. The main reason is that the pore space of the aggregates was blocked up with air, which prevented liquid from entering the pore space. If the air in the inner pores of the porous materials is evacuated before immersion, the aggregates can absorb large quantity of liquid. As shown in the fifth column of Table 2, up to 72.5% of water was absorbed by the porous aggregates after vacuum evacuation.

Table 2
Basic properties of porous materials

	Density (g/cm^3)	Porosity (MIP) (%)	Water-absorbing capacity by simple immersion (%)	Water-absorbing capacity by vacuum impregnation (%)
C1	0.76	75.6	11.0	72.5
C2	1.25	41.9	5.9	42.5
S	1.39	33.8	4.1	15.0

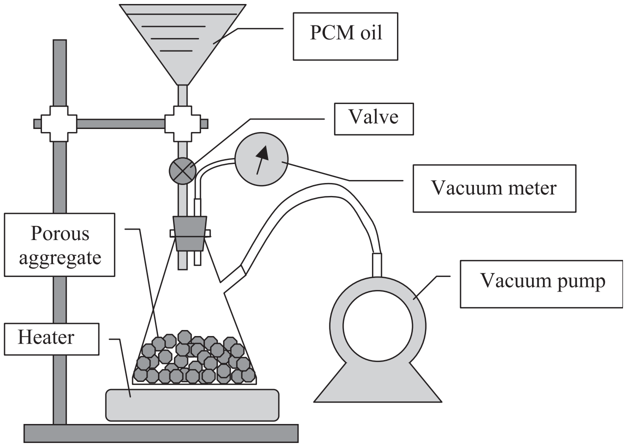

Fig. 2. Schematic drawing of the vacuum impregnation setup.

In the PCM absorption process of porous aggregates, vacuum evacuation was used. Fig. 2 shows a schematic drawing of the setup of the absorption process. Porous aggregates were placed inside a flask, which was connected to a vacuum pump, a vacuum meter, and a container of liquid PCM.The connecting joints of the system were sealed with vacuum grease. The vacuum pump was used to evacuate air from the porous aggregates, and the vacuum meter to monitor the vacuum pressure of the system. The evacuation process continued for about 30 min at vacuum pressure of 88.1 kPa. Then, the valve between the flask and the container of liquid PCM was turned open, and liquid PCM was allowed to flow into the flask to the level covering all aggregates. Finally, operation of the vacuum pump was stopped, and air was allowed to enter the flask again to drive liquid PCM to penetrate into the pore space of aggregates. After about 30 min, the aggregates were taken out of the flask and cleaned with a cotton towel.

The PCM-absorbing results in the porous materials are shown in Table 3.

Table 3
PCM-absorbing capacity of the porous materials

	C1	C2	S
PCM-absorbing capacity (%)	68.0	15.0	6.7

Table 4
Concrete mix proportions

	Water (kg/m^3)	Cement (kg/m^3)	Sand (kg/m^3)	Coarse aggregate (kg/m^3)
NC	170	340	583	1325
C1	212	340	583	380
C2	208	340	583	625
S	198	340	583	695
OC1	170	340	583	638
OC2	170	340	583	719
OS	170	340	583	744

NC, C1, C2, S, OC1, OC2, and OS, stand for normal concrete and concretes containing C1, C2, S, OC1, OC2, and OS aggregates, respectively.

2.2.2. Thermal energy storage concrete

TESC was made from Portland cement, sand, TESAs, and water. For comparison, normal concrete and concrete with plain porous aggregates were also prepared. OC1, OC2, and OS were used to denote concretes made with TESAs that are C1, C2, and S porous aggregates with incorporation of PCM. The concrete mix proportions are listed in Table 4.

2.3. Materials characterizations

2.3.1. Pore structure of the porous aggregates

To elucidate the reasons for the difference in the PCM-absorbing capability between different porous aggregates, two methods, mercury intrusion porosimetry (MIP) and image analysis (IA), were used to characterize the porous structure of these materials.

2.3.2. Thermal test

Normal concrete and TESCs were crushed to coarse powders, which were subjected to differential scanning calorimetry (DSC) analysis to evaluate their thermal energy storage capacity. DSC sample weight was around 70 mg.

3. Results and discussion

3.1. Porous structure

3.1.1. Results of MIP test

Fig. 3 shows the MIP test results of the three kinds of porous materials. Three interesting points were found.

(1) The porosity of C1 aggregate is much larger than that of the other two kinds of porous materials, and the porosity of C2 is slightly larger than that of S. This partly explains the difference of the liquid absorbing capability between these porous materials (Fig. 3a).

(2) It is easy to find the similarity between cumulative pore volume curves of C1 and C2 and the dissimilarity between the curves of the expanded clay materials and expanded shale material (Fig. 3a). The increment of the pore volume of expanded shale material is almost linear with the decrease of the pore diameter. There are two rapidly increasing phases on the cumulative pore volume curves of expanded clay materials in the pore diameter ranges from 1 to 10 μm and from 0.1 to 1 μm. These two phases correspond to two main peaks on the incremental pore volume curves of expanded clay materials (see Fig. 3b).

(3) A rough estimation of the penetrating degree of the liquid PCM into the porous materials can be made based on the cumulative pore volume curves, absorption data in Tables 2 and 3 and density of PCM in Table 1. For C1 material, the volume of liquid PCM absorbed by 1 g of porous material is 0.68/0.85 = 0.786 ml. In Fig. 3a, it can be seen that the diameter of pore reached by liquid PCM corresponding to this volume is about 0.4 μm. By the same method, the volume of liquid PCM absorbed by 1 g of C2 and S is 0.176 ml and 0.081 ml, respectively, and the minimum diameter of pore reached by the liquid PCM is about 1.0 and 1.5 μm for C1 and S, respectively. If we consider the volume space of the pore with diameter above 0.01 μm as the total pore space of the materials, then we can estimate the volume occupation ratio (VOR) of liquid PCM

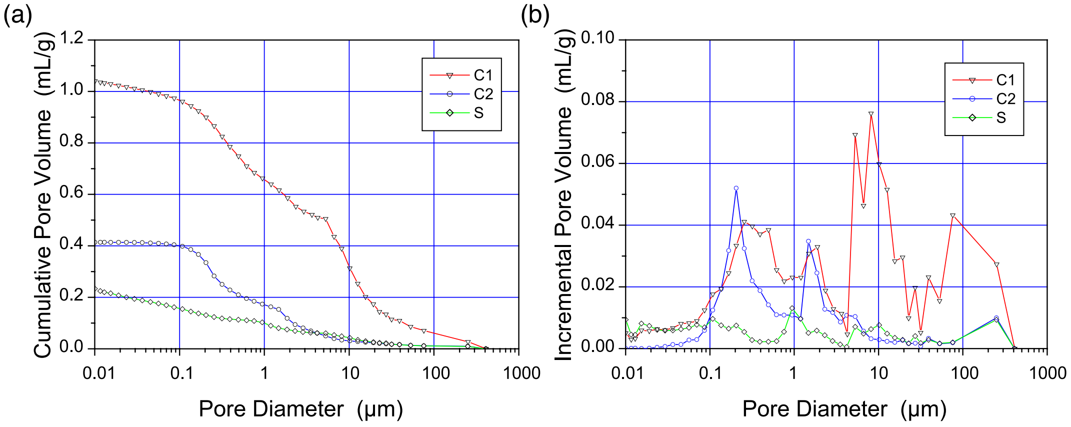

Fig. 3. MIP results of the three kinds of porous materials.

Table 5
Penetration degree of liquid PCM in different porous materials

	C1	C2	S
MPDR (μm)	0.4	1.0	1.5
VOR (%)	75.6	41.9	33.8

in the porous materials, which is 75.6%, 41.9%, and 33.8% for C1, C2, and S, respectively. The above analysis is summarized in Table 5.

3.1.2. *Influence of viscosity*

Fig. 4 depicts the absorbing behavior of the porous materials at different conditions (simple immersion and vacuum impregnation) and for different liquids (water and PCM). The shape of curves in this figure is similar to that of the cumulative pore volume curves in Fig. 3a. This implies that different liquids under different pressures can reach pore space with different diameters. First, due to the lower viscosity of water in comparison with PCM (0.9 cP for water and 7 cP for PCM), water can penetrate into pore space with smaller diameter and occupy more pore space than PCM in the same porous material and at the same vacuum pressure. Second, for the same liquid, different pressures can bring the liquid to different void levels and occupy different volumes of the porous structure.

3.1.3. *IA results*

The VOR of liquid PCM in the porous materials and minimum pore diameter reached (MPDR) by PCM are related to the features of the pore geometry of the porous materials, which cannot be fully characterized by MIP test alone. IA of optical microscopic (OM) or scanning electron microscopic (SEM) images can provide complementary information for the study of MIP results.

Fig. 5 shows examples of OM images of C1, C2, and S. A, C, and E are images of the inner part of C1, C2, and S materials, respectively; B, D, and F are the images of the boundary part of C1, C2, and S materials, respectively. In the images, white portions represent pore. By binary process and pixel calculation, the porosity of different parts of the materials can be obtained. Table 6 gives statistical features of the porous structure extracted from OM images. The connectivity factor of the porous structure is defined as the ratio of the area of the biggest pore to the total pore area in an image. Data in Table 6 are average values of the analysis results of more than five images.

The OM observation of the porous structure of the porous materials and IA analysis can provide useful information for us to understand the absorbing behavior of these materials, which are described in detail in the following paragraphs.

3.1.3.1. Porosity and transport tunnel in boundary part. It is clear that the porosity of the boundary part of C2 and S materials is lower than that of C1 materials (see Table 6 and Fig. 5B, D, and E). Additionally, there exists a continuous transport tunnel in the boundary part of C1 material, as shown in Fig. 5B. It is difficult to find obvious transport tunnel in boundary parts of C2 and S materials (Fig. 5D and F). Higher porosity and continuous transport tunnel in the boundary part allow larger amount of liquid PCM to penetrate into the porous space of C1 material than C2 and S materials.

3.1.3.2. Connectivity of porous structure. Another important feature of the porous geometry affecting the absorbing behavior of porous materials is the connectivity of the porous structure. It can be clearly seen in its microscopic image (Fig. 5A) that the pores of C1 material are highly interconnected, with a high connectivity factor of 0.98. This means that a large part of the inner pore space of C1 material can be easily reached and occupied by liquid PCM. On the contrary, the connectivity factor of C2 material is relatively lower than that of C1; about half of the pore space is interconnected, as shown in its microscopic image (Fig. 5C). In addition, if we look at the microscopic image of S materials (Fig. 5E), we can find that the pores are basically isolated and unconnected. Its connectivity factor is only 0.2, which is very low in comparison with that of the expanded clay porous materials.

3.2. *Thermal energy storage capacity*

The thermal energy storage capacity was evaluated by means of DSC test. Concrete samples were crushed and well mixed to coarse powders, which were used to conduct DSC test. Fig. 6 shows the DSC curves of the normal concrete material, concrete materials made with porous aggregates with or without PCM. It can be seen in the figure that DSC

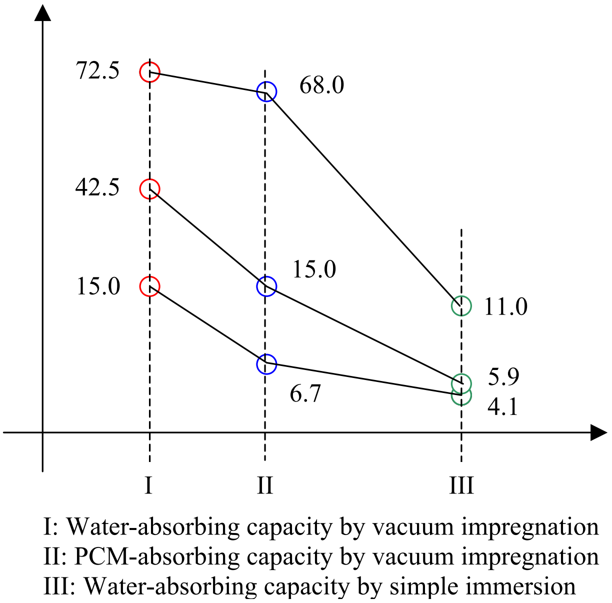

Fig. 4. Absorbing behaviors of the porous materials.

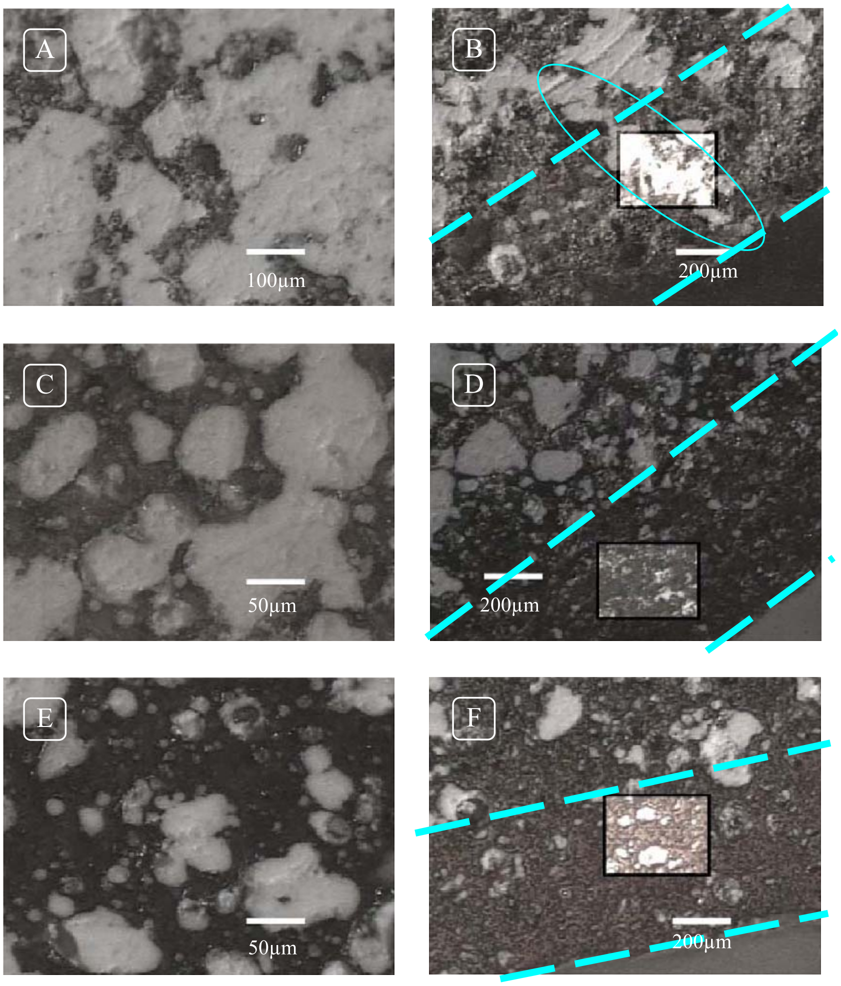

Fig. 5. OM images of porous materials.

curves of NC, C1, C2, and S specimens are straight lines, while the curves of OC1, OC2, and OS specimens all have endotherm peaks.

Fig. 6 also shows a DSC curve with hollow square symbol for a commercially available plastic PCM, which is usually used as thermal buffer material for electronic components of computers. It is plotted here for comparison. It can be seen that concrete samples made of porous aggregate (C1 and C2) with PCM (butyl stearate) have similar thermal energy storage capacity with that of commercial plastic PCM.

The DSC curve of butyl stearate is also superimposed in Fig. 6. It can be observed that its phase changing range is from 10 to 30 °C. It should be noted that there are two endotherm peaks in the DSC curve of butyl stearate, which means that there are at least two components within the material. In other words, the butyl stearate we selected

Table 6
Statistical features of microstructure of porous materials from IA

	C1	C2	S
Porosity (%)			
Inner part	65.0	53.3	30.7
Boundary part	39.4	12.7	16.7
Boundary thickness (μm)	546.4	583.5	536.0
Connectivity factor	0.98	0.64	0.20

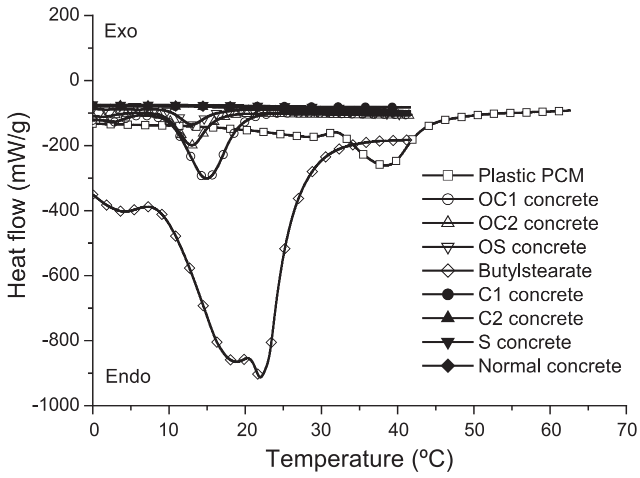

Fig. 6. DSC curves of different materials.

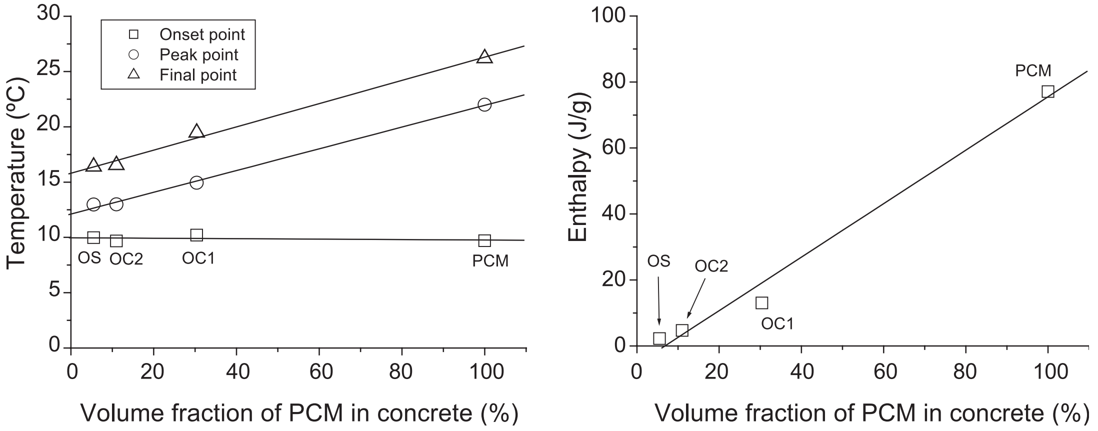

Fig. 7. Thermal behavior versus volume fraction of PCM.

is not pure. Materials with a high degree of purity have a narrower phase changing range, but also a higher price. For reasons of economy, which should be considered in the research and development of new building materials, it is not applicable to use materials with high purity. Therefore, an inexpensive industrial product of butyl stearate with a wider phase changing range was chosen in this study to make a proper balance between performance and economy of the final product.

Fig. 7 shows the relationship between the phase changing parameters and the volume fraction of PCM in concrete. Some interesting phenomena can be found in Fig. 7. First, the phase changing temperatures are affected by the volume fraction of PCM in concrete in different ways. The onset temperature of the phase changing almost does not change for different volume fractions of PCM in concrete, but the peak and ending temperatures of the phase changing increase linearly with the volume fraction of PCM in concrete. It is supposed that the porous structure of the supporting materials affects the phase changing behavior of the PCM. The enthalpy of phase changing increases almost linearly with the volume fraction of PCM in concrete, which can be easily understood.

4. Conclusions

The following conclusions can be drawn from the current study.

(1) Porous aggregates, such as expanded clay and shale, can be used as supporting materials of PCMs and used to produce TESC for the indoor temperature control of modern buildings and improvement of building energy efficiency.

(2) By comparing the results of MIP test and absorbing behavior of PCM in the porous materials, it can be estimated that the PCM can penetrate into pore space with diameter of 1 to 2 μm and occupy up to 75% of the total pore space of the porous materials.

(3) The results of IA indicate that the geometrical features of porous structure, including porosity, transport tunnel in boundary part and connectivity factor of the pore structure of the inner part, greatly affect the PCM-absorbing behavior of the porous materials.

(4) The phase changing behavior is significantly affected by the volume fraction of PCM in the concrete. The peak and ending temperatures and the enthalpy of phase changing increase linearly with the volume fraction of PCM, but the onset temperature of the phase changing almost does not change.

(5) It can be found from the results of DSC test that the thermal energy storage capacity of TESC produced by the two-step method is comparable with that of one commercially available PCM product. This means that the two-step method proposed in this paper is feasible and has potential application in the field of building energy conservation.

Acknowledgements

This work was sponsored by the National Natural Science Foundation of China (50208015), National Key Fundamental Research Program (2001CB610705-01), Shanghai Raising-Star Program (03QF14050) and Shanghai Nanotechnology Project (0352nm033).

References

[1] Y. Hirayama, S. Jolly, W.J. Batty, Investigation of thermal energy storage within building thermal mass in northern Japan through dynamic building and building services simulation, Proceedings of the 7th International Conference on Thermal Energy Storage, Japan, 1997, pp. 355–360.

[2] I. Dincer, M.A. Rosen, Thermal Energy Storage, Wiley, Chichester, UK, 2002.

[3] H.J. Strumpf, M.G. Coombs, Solar receiver for the space station Brayton engine, J. Sol. Energy Eng. 110 (4) (1988) 295–300.

[4] Q.D. Wang, X.Y. Zhang, H.B. Kang, Selection of phase changing

composites, Journal of Beijing Institute of Light Industry 15 (1) (1997) 61–65 (in Chinese).

[5] Y.Q. Zhang, State of the art of the thermal energy storing air-conditioner, New Technologies in Heating, Ventilating & Air Conditioning 1 (1) (1999) 10–15 (in Chinese).

[6] I.O. Salyer, Thermal energy storage, Proceedings of DOE Energy Storage Research Activities, New Orleans, 1989, pp. 97–110.

[7] Y.P. Zhang, Y.B. Kang, Y. Jiang, Research of the application of the phase changing energy storage and chemical reaction energy storage for heating, ventilating and air conditioning of buildings, Heating, Ventilating & Air Conditioning 29 (5) (1999) 34–37 (in Chinese).

[8] Y. Ryu, T. Watanabe, Y. Yoshitake, Y. Akashi, M. Hashimoto, A study on environmental characteristics of the air-conditioning system with floor thermal storage, Proceedings of the 7th International Conference on Thermal Energy Storage, Japan, 1997, pp. 361–366.

[9] K.A.R. Ismail, J.N. Castro, PCM thermal insulation in building, Int. J. Energy Res. 21 (14) (1997) 1281–1296.

[10] Z.R. Li, Analysis of the heat transfer of energy storing structures, Journal of Tongji University 29 (3) (2001) 338–341 (in Chinese).

[11] Z.R. Li, Z.W. Chen, Study on the heat transfer through PCM-wallboard, Proceedings of International Conference on Energy Storage Cooling Technology, Shanghai, 2001, pp. 46–52.

[12] M.M. Shapiro, D. Feldman, D. Hawes, D. Banu, PCM thermal storage in wallboard, Passive Sol. J. 4 (4) (1987) 419–439.

[13] R.J. Kedi, Conventional wallboard with latent heat storage for passive solar application, Proceedings of the 25th Intersociety Energy Conversion Engineering Conference (IECEC-90), Reno, NV, 1990, pp. 222–225.

[14] D. Feldman, D. Banu, D. Hawes, A. Athienitis, C. Liu, Energy storage building materials with organic PCM's, Proceedings of the 28th Intersociety Energy Conversion Engineering Conference, Atlanta, 1993, pp. 143–148.

[15] I.O. Salyer, A.K. Sircar, Development of phase change technology for heating and cooling of residential buildings and other applications, Proceedings of the 28th Intersociety Energy Conversion Engineering Conference (IECEC-93), Atlanta, 1993, pp. 133–142.

[16] D. Hawes, J. Paris, D. Feldman, D. Banu, Heat storage and energy conservation in buildings, Proceedings of the 2nd International Energy Congress, Morocco, 1995, pp. 127–130.

[17] D.K. Mao, Energy storing composites containing phase changing material, New Energy 19 (11) (1997) 7–10 (in Chinese).